

## Transport of Ions and Solvent in Confined Media

Albert Lehmani,<sup>1</sup> Olivier Bernard,<sup>1</sup> and Pierre Turq<sup>1,2</sup>

*Received November 15, 1997; final June 11, 1997*

---

A new theoretical approach is used to model the transport properties of a cation-exchange membrane. By using the Navier–Stokes equation related to the Poisson–Boltzmann relation, it is thus possible to determine the solvent velocity in a membrane pore, and the influence of electroosmosis on the transport properties of the polymer. The variation of the transport coefficients with salt concentration in the membrane pore was modeled as for simple electrolytes: taking electrophoretic interactions and relaxation effect into account, we used MSA analytical expressions. We have investigated membrane conductivity and electrophoretic sodium mobility measurements when the membrane was equilibrated with NaCl solution. Good agreement was found between the experimental results and our theoretical model.

---

**KEY WORDS:** Ion-exchange membrane; transport properties; electroosmosis; Poisson–Boltzmann equation; MSA theory.

---

### 1. INTRODUCTION

Ion-exchange membranes play a vital role in a number of electrochemical devices and in numerous areas of life sciences,<sup>(1)</sup> including batteries,<sup>(2,3)</sup> fuel cells,<sup>(4)</sup> electrochemical sensors and electrochemical reactors.<sup>(5–8)</sup> The need to predict accurately the membrane transport rates of solute and solvent has become more and more important since the last decade.<sup>(9–13)</sup> Moreover, in spite of their importance, scientists do not fully understand the behaviour of mobile species within ion-exchange membranes.<sup>(14–26)</sup> A variety of mathematical models have been elaborated in order to describe transport in confined media. Two fundamental approaches are in current

---

<sup>1</sup> Laboratoire d'Electrochimie URA CNRS 430, Université Pierre et Marie Curie, 75252 Paris Cedex 05, France.

<sup>2</sup> To whom correspondence should be addressed.

usage: the Nernst–Planck flux equations<sup>(27, 28)</sup> and extensions thereof, and the theory of irreversible thermodynamics.<sup>(29–31)</sup> The limitation of the first approach is the requirement for detailed knowledge about the structure and the thermodynamics properties of the membrane, and is only available for dilute systems. The second approach consists of a phenomenological description of the membrane-solute-solvent system. This method can be used to describe the magnitude and coupling between various transport processes, but requires an important number of transport parameters like friction coefficients, which represent the physical interactions between ions and the membrane.

In this paper, a new theoretical approach is proposed to analyse the variation of the membrane conductivity with the external electrolyte concentration. This macroscopic parameter is not only dependent on the electroosmotic flow of water in the membrane but also on the cations and anions mobilities which are present in the polymer. Therefore we need two theoretical models in order to take both of these physical phenomena into account. First, we consider the membrane as an array of parallel cylindrical pores of constant radius, and with a uniform distribution of ion-exchange sites on the pores walls. Then we use the Poisson–Boltzmann equation in order to determine the electric potential and ion concentration profiles in the radial pore direction. By using the Navier–Stokes equation for the axial fluid velocity in the membrane pore, we can thus deduce the electroosmotic mobility and its influence on the membrane conductivity. This approach is often used in various electrokinetic transport studies<sup>(9)</sup> but the aim of our processes is quite original.

In the following of this study, we must take the cations and anions mobilities in the membrane into account. As for simple electrolytes,<sup>(46, 47)</sup> we assume that ions have a mobility when the added salt concentration becomes very low. In that case, the membrane pores are only filled with solvent and counterions (cations) of mean mobility. We assume that this one does not vary with the electrolyte concentration and that the added ions are not associated with the fixed charges of the membrane. In order to describe the variation of the added ions mobilities with the salt concentration, we must take the electrophoretic interactions and the ionic atmosphere relaxation into account. These phenomena can be properly solved in the framework of the Mean Spherical Approximation (MSA)<sup>(48, 49)</sup> introduced in the Fuoss–Onsager transport theory.<sup>(55)</sup>

In this paper, we focused on the study of the transport properties of the Nafion 117 membrane, manufactured by E. I. du Pont de Nemours & Company. This kind of perfluorosulfonic acid cation exchange membrane has been used frequently in experimental and transport studies,<sup>(10, 32–43)</sup> and its microstructure is relatively well understood. According to Gierke,<sup>(44)</sup>

Nafion membrane is described as a series of clusters or inverted micelles, interconnected by narrow pores. Physical measurements including x-ray diffraction and neutron scattering showed that the cluster diameters vary with membrane equivalent weight and range from 30 to 60 Å.

Cation-exchange membranes in contact with an external electrolyte absorb ions and solvent in a manner different from that of neutral membranes.<sup>(45)</sup> They partially exclude co-ions (anions) by electrostatic repulsion because of the presence of ionic fixed-charged groups ( $SO_3^-$ ) in the polymer matrix. The overall transport characteristics of the membrane are dependent on the cations and anions concentration which are absorbed in the polymer matrix, and also on the membrane porosity and the solvent content. It is thus necessary to obtain all these experimental parameters in order to model the transport properties of the membrane.

In this work, the transport characteristics of the Nafion 117 membrane have been first determined with conductivity measurements when the membrane was equilibrated with NaCl solution by varying the electrolyte concentration and the temperature. We have also determined the electric mobility of sodium ion in the membrane with an electrophoresis technique. By using the transport theories described above, we can thus model the variation of the sodium mobility with the salt concentration in the membrane. In the first part of this paper we give an evaluation of the electroosmotic contributions as excess properties and take into account the departures from ideality (excess properties) as an effect of the coulomb forces on the motion of ions and solvent.

The effect of coulomb forces is calculated in a standard way by a Poisson-Boltzmann equation, and the effect of those forces on solvent and ion transport is evaluated à la Smoluchowski by a Navier-Stokes equation.

The total ionic mobility is expressed as a sum of an electroosmotic term, calculated as indicated above, plus an intrinsic term, containing also departures from ideality. For high concentrations in which the screening length of the density correlations  $\kappa^{-1}$  is smaller than the diameter of the pores, the MSA approximation is a first approximation of non ideality even in transport (54), (55).

## 2. THEORETICAL SECTION

### 2.1. Ionic Distribution in the Membrane

Nafion membranes are generally described as a series of clusters or inverted micelles, interconnected by narrow pores. The distribution of surface charge density between the clusters and the narrow pores and the exact form of these clusters and pores are not well known. In order to

describe thermodynamic properties of the ions in the membranes, a spherical model of clusters seems to be a good first approach. But for transport properties we need of an open subunit to calculate not only the distribution of ions in the vicinity of the pore walls but also the solvent and ions velocities inside the cavities. Spherical or other closed form of cavities would give unrealistic results for the velocities. A cylindrical model of pores seems to be the simpler which permits to take into account these characteristics.

Then we consider the membrane as an array of parallel cylindrical pores of constant radius  $a$  and of length  $L$ , with a uniform distribution of ion-exchange sites on the pores walls. When there is no added salt in the membrane, it contains counterions ( $m$ ) required for neutralizing the charged sites with concentration  $\bar{X}$ , expressed in number of moles per unit volume of wet membrane. This quantity is obtained from the ion-exchange capacity (IEC) determination and from swelling properties of the membrane.

The fixed cations concentration in the pores is then deduced of  $\bar{X}$  by the following relation:

$$\bar{C}_m = \frac{\bar{X}}{\tau} \quad (1)$$

In these equations,  $\tau$  is the membrane void porosity (volume of free solution within the membrane per unit volume of wet membrane) The porosity can be obtained by the following expression:<sup>(10)</sup>

$$\tau = \frac{\Delta V}{1 + \Delta V} \quad (2)$$

where  $\Delta V$  is the volume increasing of the membrane upon absorption of the electrolyte solution per unit of dry membrane volume. This quantity is also calculated from membrane water and electrolyte solution content data using the following equation:

$$\Delta V = \frac{\Delta W_h \rho_d}{\rho_e} \quad (3)$$

where  $\rho_e$  is the density of the aqueous electrolyte solution which enters into the membrane,  $\rho_d$  is the density of dry Nafion 117 polymer ( $1.98 \text{ g cm}^{-3}$ ),  $\Delta W_h$  is the ratio of mass increasing of the membrane upon absorption of the electrolyte solution to the mass of dry membrane. Using the electro-

neutrality condition, the total charge of the membrane pore is then related to the number of counterions by the relation:

$$\frac{Z_m}{L} = \bar{C}_m \pi a^2 \mathcal{N}_s \quad (4)$$

where  $\mathcal{N}_s$  is the Avogadro number. The surface charge density  $\sigma$  is also given by the relation:

$$\sigma = \frac{\bar{C}_m a \mathcal{F}}{2} \quad (5)$$

where  $\mathcal{F}$  is the Faraday constant. When the membrane is equilibrated with salt solution, the pores are filled with cations (+) and anions (−) in excess of charge  $Z_+$  and  $Z_-$  respectively. We assume that the system verifies electroneutrality with the relation for 1–1 added electrolyte:

$$\bar{C}_+^r = \bar{C}_-^r + \bar{C}_m \quad (6)$$

where  $\bar{C}_+^r$  and  $\bar{C}_-^r$  are the cations and anions concentrations in the pore. The radial distribution of the electric potential  $\Psi$  in a charged pore is determined by using the Poisson–Boltzmann equation expressed in cylindrical symmetry:

$$\Delta\Phi = \frac{1}{r} \frac{\partial}{\partial r} \left( r \frac{\partial\Phi}{\partial r} \right) = (4 \times 10^3 \pi L_B \mathcal{N}_s) \sum_i Z_i M_i \exp(Z_i \Phi) \quad (7)$$

where  $\Phi = -e\Psi/k_B T$  and  $L_B$  is the Bjerrum length defined as

$$L_B = \frac{e^2}{4\pi\epsilon_0 \epsilon k_B T} \quad (8)$$

where  $\epsilon$  is the permittivity of the solution in the pore. The dielectric constant of water in the pore was set equal to 78. The boundary conditions in the pore center are  $\partial\Phi(0)/\partial r = 0$  and  $\Phi(0) = 0$ . The  $M_i$  ( $\text{mol l}^{-1}$ ) constants are related to the average concentrations  $\bar{C}_i^r$  and integrated in the total volume of the pore:

$$\bar{C}_i^r = \frac{2M_i}{a^2} \int_0^a \exp(Z_i \Phi) r dr \quad (9)$$

In most cases, this set of equations can only be resolved numerically. Starting from an initial guess of the  $M_i$  constants, the integration of the

Poisson–Boltzmann equation is obtained by a 4th order Runge–Kutta equation, from the initial position  $r=0$ . The integrals are computed by trapezoidal integration and the  $M_i$  constants are estimated using Belloni's method.<sup>(46)</sup> The accuracy of the computation is tested by comparing the quantity  $d\Phi(a)/dr$  with the theoretical value determined from Gauss law:

$$\frac{d\Phi(a)}{dr} = -2 \frac{Z_m L_B}{L a} \quad (10)$$

The radial distribution of cations and anions concentrations in the pore is then simply deduced from the potential  $\Phi$  by the following relation:

$$C_i(r) = C_i(r=0) \exp[Z_i \Phi(r)] \quad (11)$$

In the special case of no added salt in the membrane pore, the (PB) equation can be solved analytically. The solution for the potential is:<sup>(17, 18)</sup>

$$Z_1 \Phi(r) = -2 \ln(1 - \kappa^2 r^2) \quad (12)$$

with

$$\kappa^2 = \frac{\pi}{2} L_B M_1 Z_1^2 \quad (13)$$

and

$$M_1 = \frac{\bar{C}_m}{1 + (\pi/2) L_B \bar{C}_m Z_1^2} \quad (14)$$

## 2.2. Solvent Transport

In this paragraph we take an adaptation of the classical Smoluchowski's method for electroosmosis to porous systems.<sup>(14)</sup> The solvent velocity in the membrane pore can be deduced from the Navier–Stokes equation:

$$\eta \Delta v^s = \nabla p - \vec{F} \quad (15)$$

where  $\eta$  is the solvent viscosity,  $\nabla p$  is the pressure gradient and  $\vec{F}$  is the body force per unit volume. If the solvent is incompressible  $\nabla \cdot \vec{v}^s$  vanishes. Along the radial axis, we have:

$$\frac{\partial p}{\partial r} - F_r = 0 \quad (16)$$

which corresponds to electrostriction; and along the longitudinal axis, we have:

$$\eta \Delta v_z^s = \frac{\partial p}{\partial z} - F_z \quad (17)$$

A contribution to the solvent velocity,  $v^s$ , is due to the movement of ions within the membrane pore. So the electric force  $F_z$  is dependent on the ionic distribution of ions in the membrane:

$$F_z \simeq \mathcal{N}_A \times 10^3 \sum_j M_j e Z_j E_z \exp(Z_j \Phi) \quad (18)$$

where  $E_z$  is the electric field. By using the (PB) equation (Eq. 8) and the Navier–Stokes equation (Eq. 18), the solvent velocity is expressed as:

$$\Delta v^s = \frac{-e E_z}{4\pi\eta L_B} \Delta \Phi \quad (19)$$

By integrating along the radial axis and supposing that the solvent velocity is equal to zero at the pore wall, we obtain:

$$v^s(r) = \frac{-e E_z}{4\pi\eta L_B} [\Phi(z) - \Phi(r)] \quad (20)$$

The profile of the electroosmotic mobility  $u^s$  is then given by the relation:

$$u^s(r) = \frac{-e}{4\pi\eta L_B} [\Phi(a) - \Phi(r)] \quad (21)$$

### 2.3. Membrane Conductivity

In order to compute the ionic conductivity in the membrane pore,  $\chi_m^r$ , we must calculate the following quantity:

$$\chi_m^r = \mathcal{F} \sum_i \bar{C}_i^r Z_i \hat{u}_i \quad (22)$$

where  $\hat{u}_i$  is the mean mobility of the  $i$  ion, related to the mean velocity by  $\hat{u}_i = \hat{v}_i / E_z$ , and  $\mathcal{F}$  is the Faraday constant. We define the local velocity  $v_i$  of the  $i$  ion by the relation:

$$v_i = Z_i u_i e E_z + v^s \quad (23)$$

By taking the (PB) definition of the local concentration  $C_i(r)$ , and assuming as a first approximation that the ionic mobilities  $u_i$  are constant with the position, we have:

$$\sum_i C_i(r) Z_i v_i = \sum_i M_i Z_i \exp(Z_i \Phi) [Z_i u_i e E_z + v^s] \quad (24)$$

By integrating on the pore volume, we deduce the mean value of this quantity:

$$\sum_i \frac{\int_0^a r C_i(r) Z_i v_i dr}{\int_0^a r dr} = \sum_i \bar{C}_i^r Z_i [Z_i u_i e E_z + \hat{v}^s] \quad (25)$$

with

$$\hat{v}^s = \frac{\int_0^a v^s \exp(Z_i \Phi) r dr}{\int_0^a \exp(Z_i \Phi) r dr} \quad (26)$$

The mean velocity of the  $i$  ion is then given by the relation:

$$\hat{v}_i = Z_i e E_z u_i + \hat{v}^s \quad (27)$$

By using Eq. (23), the membrane pore conductivity can be written as:

$$\chi_m^r = \chi_i + \chi_s \quad (28)$$

where  $\chi_i$  is the ionic conductivity in the pore and  $\chi_s$  is the electroosmotic part of the conductivity in the membrane pore, which is defined as:

$$\chi_s = \mathcal{F} \sum_i \bar{C}_i^r Z_i \hat{v}^s \quad (29)$$

Now, in order to describe the experimental variations of the membrane conductivity with the electrolyte concentrations we also need a theoretical model for the mean mobilities of the ions. We consider that the membrane ionic conductivity is dependent on the counterion mobility and on the free ions (cations and anions) mobilities within the membrane pore. Therefore the conductivity  $\chi_m^r$  can be written as:

$$\chi_m^r = \chi_o + \sum_i \bar{C}_i^r \lambda_i + \chi_s \quad (30)$$

where  $\chi_o$  is the conductivity due to the counterion defined as:

$$\chi_o = \bar{C}_m \lambda_m \quad (31)$$



and  $\lambda_m$  is the ion conductivity of the counterion. The ionic conductivities  $\lambda_i$  are related to the mobilities of the  $i$  ions by the relation:

$$\lambda_i = Z_i e u_i \quad (32)$$

As for simple electrolytes and polyelectrolytes, we assume that ions have a conductivity  $\lambda_i^\circ$  when the added salt concentration in the membrane pore becomes very low. In that case, the membrane pores are only filled with solvent and counterions of mean mobility  $\lambda_m$ . In fact, most of these counterions are close to the pore wall. Then, for hydrodynamic and electrostatic reasons, the mobility of these counterions must be lower than the values known in simple electrolytes. The free ions within the pore must also have a lower mobility.

The strong coulombic interaction between the fixed charges on the pore wall and the counterions leads to the "condensation" of some fraction of cations in the vicinity of these fixed charges. Therefore we assume that the counterion mobility does not vary with the electrolyte concentration and that the added ions are not associated with the fixed charges of the membrane.

In order to describe the variation of the ionic conductivities  $\lambda_i$  of the free ions, we must take the electrophoretic interactions and the ionic atmosphere relaxation into account, as for simple electrolytes. We recently obtained new extended laws for the variation with concentration of transport coefficients of strong and associated electrolytes.<sup>(55)</sup> Our work was based on modern equilibrium pair distribution functions and the Fuoss–Onsager transport theory. For the equilibrium pair distribution function we used either the HNC (Hypernetted Chain) approximation or the MSA which leads to analytical expressions. The basic equations of the relaxation effect are the hydrodynamic continuity equations which relate the two particle density  $f_{ij}$  with velocity  $v_{ij}$  of an ion  $j$  in the vicinity of an ion  $i$ .

$$-\frac{\partial f_{ij}}{\partial t} = \text{div}_1(f_{ij}\vec{v}_{ij}) + \text{div}_2(f_{ji}\vec{v}_{ji})$$

For homogenous solution of electrolytes the two particle density are expressed as product of one-particle densities and pair distribution function:

$$f_{ij}(\vec{r}_1, \vec{r}_2) = \rho_i(\vec{r}_1) \rho_j(\vec{r}_2) g_{ij}(\vec{r}_1, \vec{r}_2)$$

In the linear response theory, the pair distribution functions are then expressed as the sum of an equilibrium part (superscripts  $^\circ$ ) and a part that

is proportional to the external perturbation (superscript'). For conductance the external force is an electric field. In confined media, this formalism can be used to compute the variation of the ionic conductivities in a region where  $\rho_i(\vec{r}_1)$  is slowly varying compared to the range of molecular correlations. Moreover  $g_{ij}(\vec{r}_1, \vec{r}_2)$  will then take the form  $g_{ij}(\vec{r}_1 - \vec{r}_2)$ . That is the case for a high concentration range of the added salt in the membrane. In fact, for a low concentration range, the variations of the ion conductivity are not very important.

The ion conductivity of the  $i$  ion can be written as:

$$\lambda_i = \lambda_i^\circ \left( 1 + \frac{\Delta u_i}{u_i^\circ} \right) \left( 1 + \frac{\Delta E}{E} \right) \quad (33)$$

where  $\Delta u_i/u_i^\circ$  is related to the electrophoretic correction and  $\Delta E/E$  is related to the relaxation effect. The quantity  $\Delta u_i$  is determined from the relation:<sup>(54)</sup>

$$\Delta u_i = \sum_j \rho_j e Z_j \int_0^\infty (g_{ij}(r) - 1) \vec{T} \vec{E} \, dr \quad (34)$$

where  $\rho_j$  is the density of the  $j$  ion,  $g_{ij}(r)$  is the pair distribution function between the  $i$  and  $j$  ions,  $\vec{E}$  is the electric field and  $\vec{T}$  is the Oseen tensor defined as:

$$\vec{T} = \frac{1}{8\pi\eta r} \left( \vec{I} + \frac{\vec{r} \otimes \vec{r}}{r^2} \right) \quad (35)$$

where  $\vec{I}$  is the unit tensor. Then Eq. (35) becomes:

$$\Delta u_i = \frac{2}{3\eta} \sum_j \rho_j e Z_j \int_0^\infty (g_{ij}(r) - 1) r \, dr \quad (36)$$

The above integral is calculated by using the pair distribution functions from the MSA theory. Then we obtain the following equation:<sup>(54)</sup>

$$\frac{\Delta u_i}{u_i^\circ} = - \frac{k_B T}{3\pi\eta D_i^\circ} \frac{\Gamma}{1 + \Gamma\sigma_a} \quad (37)$$

where  $D_i^\circ$  is the diffusion coefficient of the  $i$  ion at infinite dilution, which is related to the mobility by the Nernst-Einstein relation:

$$\frac{D_i^\circ}{D_i^\circ} = \frac{k_B T}{Z_i e} \quad (38)$$

$\sigma_a$  is the mean diameter of the added ions and  $\Gamma$  is the inverse of the correlation length in the MSA theory given by:

$$4\Gamma^2(1 + \Gamma\sigma_a)^2 = \kappa^2 \quad (39)$$

with

$$\kappa^2 = \frac{4\pi e^2}{\epsilon k_B T} \sum_j \rho_j Z_j^2 \quad (40)$$

The relaxation effect is determined from the continuity relation of Onsager by using the pair distribution functions from MSA theory. So we have:

$$\Delta h'_{ji} - \kappa_q^2 h'_{ji} = \frac{Z_i e D_i^\circ - Z_j e D_j^\circ}{k_B T (D_i^\circ + D_j^\circ)} \text{EV} g_{ji}^\circ \quad (41)$$

with

$$\kappa_q^2 = \frac{e^2}{\epsilon k_B T} \frac{\rho_i Z_i^2 D_i^\circ + \rho_j Z_j^2 D_j^\circ}{D_i^\circ + D_j^\circ} \quad (42)$$

In Eq. (42),  $h'_{ji}$  is the correlation function, related to a first-order perturbation of the equilibrium. By using the equilibrium functions at the MSA level, the relaxation term is expressed as:<sup>(55)</sup>

$$\frac{\Delta E}{E} = \frac{-\kappa_q^2 e^2 |Z_i Z_j|}{6\epsilon k_B T \sigma_a (1 + \Gamma\sigma_a)^2 \kappa_q^2 + 2\Gamma\kappa_q + 2\Gamma^2 [1 - \exp(-\kappa_q\sigma_a)]} \frac{1 - \exp(-2\kappa_q\sigma_a)}{1 - \exp(-\kappa_q\sigma_a)} \quad (43)$$

Taking into account that  $\kappa_q\sigma_a$ , as well as  $\kappa\sigma_a$ , and  $\Gamma\sigma_a$  are much smaller than unity yields the relaxation term at high dilution:

$$\frac{\delta E}{E} \simeq \frac{e^2 |z_i z_j|}{3\epsilon k_B T} \left( \frac{\kappa_q^2}{\kappa_q + \kappa} - \kappa_q^2 \sigma_a + \mathcal{O}(c^{3/2}) \right) \rightarrow \frac{-\kappa_q^2 e^2 |z_i z_j|}{3\epsilon k_B T (\kappa_q + \kappa)} \quad (44)$$

For the electrophoretic term, we use the limit  $\Gamma \simeq \kappa/2 - \kappa^2\sigma_a/4$ ,

$$\frac{\delta u_i^0}{u_i^0} \simeq -\frac{k_B T}{6\pi\eta D_i^0} (\kappa - \kappa^2\sigma_a + \mathcal{O}(c^{3/2})) \rightarrow -\frac{k_B T \kappa}{6\pi\eta D_i^0} \quad (45)$$

and we recover Onsager's limiting law.

## 2.4. Cation Mobility

The theoretical model presented above allows to determine the ionic mobilities at infinite dilution of the counterion and of the free cations and anions within the membrane pore. It is thus possible to model the experimental variation of the cation mobility in the membrane which was obtained by electrophoresis experiments. When the membrane is equilibrated with electrolyte, the experimental sodium mobility is then dependent on the mobility  $u_m$  and on the mobility of the free cation  $u_+$ . We can thus write the theoretical cation mobility as follows:

$$u_{ih}^+ = \frac{\bar{C}_m u_m + \bar{C}_i^r u_+}{\bar{C}_m + C_+^r} \quad (46)$$

## 3. EXPERIMENTAL SECTION

### 3.1. Equilibrium Experiments

Before any measurement, a pretreatment of the membrane was carried out in order to expel impurities. The membranes samples were immersed successively in aqueous hydrochloric acid (Prolabo, 35%)  $1 \text{ mol l}^{-1}$  for 24 hours, deionized water for 2 hours and in sodium hydroxide (Prolabo, Normadose)  $1 \text{ mol l}^{-1}$  for 24 hours in order to exchange proton for sodium. This cycle was repeated one more time before boiling the samples for 1 hour in deionized water.

In order to get the equilibrium sodium chloride and water uptake by the membrane, we have carried out many experiments including wet density, fixed-ion concentration and membrane porosity. Moreover we have determined the membrane chloride concentration as a function of external salt concentration.

Dry membranes samples ( $3 \text{ cm} \times 3 \text{ cm}$ ) of a thickness of  $175 \mu\text{m}$ , were immersed in the electrolyte solution, e.g., sodium chloride (SDS, analytical grade) and equilibrated for 24 hours. Then, the membranes are removed from the solution and excess electrolyte was wiped from the membrane surface with filter paper. The thickness of the membrane samples was measured by means of a micrometer once the sample clamped between two thin microscopic slides. The thickness was relatively stable for a given sample: it was varying from 200 to  $190 \mu\text{m}$  when the external electrolyte concentration was increased. The weight of the membranes samples was also measured and the membrane density was determined by dividing the wet membrane weight by the wet membrane volume.

In order to get the ion exchange capacity (IEC), a membrane sample was immersed in a concentrated HCl solution for 24 h to make sure that all of the membrane charged sites were in the acid form. The membrane was then soaked in deionized water in order to remove all traces of acid. Following this, the sample was placed in a salt solution of interest and allowed to equilibrate. The salt solution must be replaced repeatedly until no extra  $H^+$  is detected in the electrolyte rinse solution. The total mole number of  $H^+$  was obtained by titration and the ion exchange capacity was calculating by dividing this number by the dry membrane weight.

The membrane chloride concentrations were found out thanks to a technique using radioactive tracers. Membrane samples were equilibrated in a NaCl solution at a given concentration for 24 hours. Then the membrane was removed from the solution, wiped with filter paper and weighed. The sample was then immersed in a NaCl solution at the same given concentration for 24 hours, in which the chloride ion is labelled with a  $^{36}Cl$  isotope (Amersham International). Afterwards, the membrane was replaced in a NaCl solution at the same given concentration for 24 hours again. The activity of this solution was measured with a Minaxi Tri-Carb 4430 (Packard Instruments)  $\beta$  counter.

### 3.2. Impedance Measurement

Conductivity measurements were made with a Plexiglass cell devised in the laboratory.<sup>(50)</sup> The cell used mercury electrodes. The wet membrane sample was clamped between two cell compartments, with an inner diameter of 9 mm, by a silicone rubber ring covered with PTFE. Two platinum wires were plunged into mercury in order to obtain impedance measurements. For both cells, the temperature was kept constant ( $\pm 0.02^\circ C$ ) by immersion of the cells into a thermostated oil bath. The measurements were performed with a Wayne-Kerr B 6425 impedance bridge in the frequency range 20 Hz–300 kHz. The amplitude of the ac voltage applied was less than 50 mV to maintain sufficient measurement accuracy. For each experiment, the membrane impedance remained stable within 1% during the time of the measurements.

### 3.3. Electric Mobility Measurement

Electric mobility of sodium ion in the membrane was performed using an electrophoresis technique. In most previous works this longitudinal method has been especially devoted to the measurement of the relative mobilities of ions (ratio of cation to anion mobilities) on a porous paper, assuming that this ratio remained constant in electrolyte solutions.<sup>(51–53)</sup>

The apparatus used to perform electrophoresis measurements, was a LKB 2117 Multiphor containing a glass plate thermostated at 5°C. This temperature was necessary to avoid the evaporation of solvent in the membrane during the experiments. The membrane sample (25 cm × 2 cm) was placed on the glass plate and each of the extremities of the sample was linked to a strip of paper in order to ensure the flow of current. Each of the papers was plunged into a compartment of 100 cm<sup>3</sup> which contained the desired electrolyte solution. Each of the compartments was linked thanks to a strip of paper to another compartment of 50 cm<sup>3</sup> containing the same solution and a platinum electrode. This experimental setting allowed the measurements not to be perturbed by the reactions occurring at the electrodes. A constant voltage was applied on the electrodes (120 V to 500 V) and the current crossing the membrane was controlled during the experiments. The membrane electric field was determined by measuring the voltage on the sample every 4 cm with a voltmeter and it was found to be quite constant with a maximum variation of 2%.

### 3. EXPERIMENTAL PROTOCOL

Samples of pretreated Nafion 117 membrane (25 cm × 2 cm) were immersed for 24 hours in sodium chloride solution. Then the samples were wiped with a filter paper and placed on the apparatus support. A drop of 10 μl of the radioactive tracer <sup>22</sup>Na (Amersham International), was put on the membrane. The sample was then covered with a strip of Parafilm, but the radioactive drops were left exposed. After 3 hours, the strip of Parafilm was removed from the membrane and the drops were wiped dry in order to avoid a surface conduction during the experiments. A plate of Plexiglass was then put on the membrane so as to prevent the solvent evaporation. The experiments were performed within one hour, and after this time, the membrane was dried at 80°C for 5 min in order to stop the diffusion process. The positions of the radioactive deposits were determined by a linear analyser β-meter Berthold LB283 coupled with a photomultiplier which allows to count β particles of very low energy.

### 4. RESULTS AND DISCUSSION

#### 4.1. Ionic Distribution and Solvent Transport

In order to determine the radial profile of the electric potential in the membrane pore, we use the experimental concentrations of sodium and chloride ions in the membrane (Table 1). One must remember that ionic concentrations in the membrane pores are obtained from water uptake

**Table 1. Experimental Parameters of the Nafion 118 Membrane as a Function of External NaCl Concentration**

| $C_e$ (mol l <sup>-1</sup> ) | $\tau$ | $\bar{C}_m$ (mol l <sup>-1</sup> ) | $\bar{C}_+$ (mol l <sup>-1</sup> ) | $a$ (Å) |
|------------------------------|--------|------------------------------------|------------------------------------|---------|
| 0.0                          | 0.3    | 4.256                              | 0.0                                | 20.00   |
| 0.05                         | 0.295  | 4.385                              | $4.48 \cdot 10^{-3}$               | 19.81   |
| 0.1                          | 0.29   | 4.47                               | 0.0127                             | 19.69   |
| 0.5                          | 0.275  | 4.745                              | 0.145                              | 19.24   |
| 1.0                          | 0.265  | 4.996                              | 0.459                              | 18.83   |
| 2.0                          | 0.25   | 5.316                              | 1.217                              | 18.34   |
| 3.0                          | 0.24   | 5.632                              | 1.909                              | 17.84   |

measurements by the membrane. Moreover we can deduce the variation of the radius pore with the external NaCl concentration, which varies from 0.05 to 3 mol l<sup>-1</sup>. In Eq. (4) we denoted  $\Delta V$  as the volume increasing of the membrane upon absorption of the electrolyte per unit of dry membrane volume. This quantity can be rewritten as:

$$\Delta V = \frac{V_w}{V_d} \quad (47)$$

where  $V_d$  is the dry membrane volume and  $V_w$  is the volume of aqueous solution in the membrane pore. This quantity is also related to the pore volume as:

$$V_w = N_p \pi a^2 a \quad (48)$$

with  $N_p$  the number of the pores and  $e$  the membrane thickness. When there is no added salt in the membrane, we define  $V_w^o$  as:

$$V_w^o = N_p \pi a_o^2 e_o \quad (49)$$

which is related to the pore radius  $a_o$  and to the membrane thickness  $e_o$  without added salt.

The variation of the radius pore with the external salt concentration is then expressed as:

$$a = a_o \left[ \frac{e_o V_w}{e V_w^o} \right]^{1/2} \quad (50)$$

In this paper, we have taken  $a_o$  equal to 20 Å, which corresponds to the cluster size in Nafion membrane.<sup>(44)</sup> We have then resolved numerically the (PB) equation by taking all the experimental parameters. In Fig. 1, we

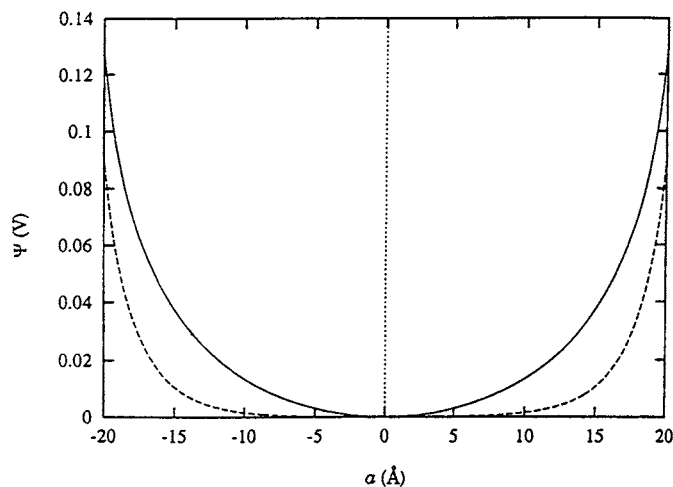


Fig. 1. Electric potential profile in a membrane pore at 25°C. (—): no salt, (---): salt concentration  $C_e$  equal to  $1 \text{ mol l}^{-1}$ .

represent the electric potential variation in the pore membrane when it is equilibrated either with water or with  $\text{NaCl } 1 \text{ mol l}^{-1}$ . We observe that the potential becomes very low in the central region of the pore, when there is excess salt in the membrane. In fact, the concentration gradient between the pore wall and the central region decreases when the salt concentration

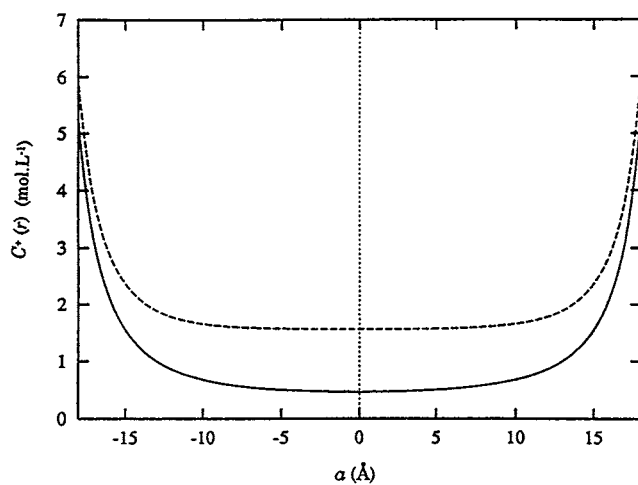


Fig. 2. Cation concentration profile in a membrane pore at 25°C. (—):  $C_e = 0.1 \text{ mol l}^{-1}$ , (---):  $C_e = 1 \text{ mol l}^{-1}$ .



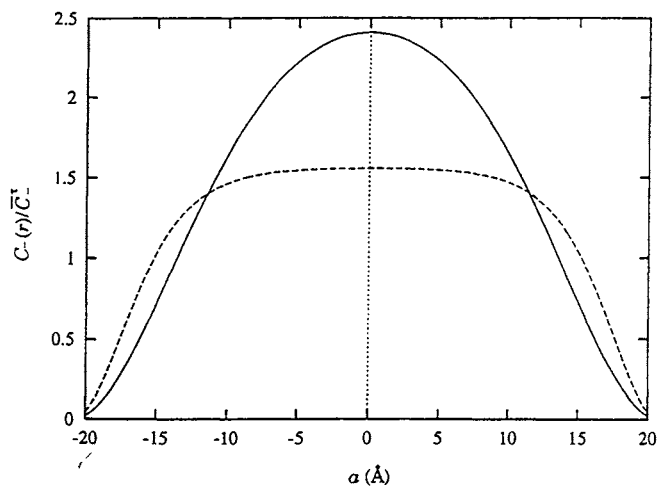


Fig. 3. Anion relative concentration profile in a membrane pore at 25°C. (—):  $C_e = 0.1 \text{ mol l}^{-1}$  (---):  $C_e = 1 \text{ mol l}^{-1}$ .

increases. Then, the ion concentration is more homogeneous within the pore, which it can be observed in Fig. 2 and Fig. 3.

In the cation concentration profile (Fig. 2), we can see a high concentration gradient which implies a high coulombic attraction of the cations near the pore wall. In the relative anion concentration profile (Fig. 3), we

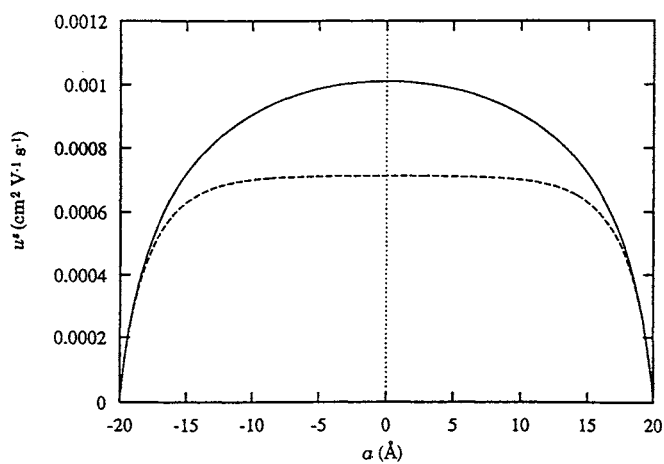


Fig. 4. Electroosmotic mobility profile in a membrane pore at 25°C. (—): no salt, (---):  $C_e = 1 \text{ mol l}^{-1}$ .

**Table 2. Simulation of the Electroosmotic Conductivity as a Function of Temperature and of Salt Concentration in the Membrane Pore**

| $C_e$<br>(mol l <sup>-1</sup> ) | $\chi_s$ (5°C)<br>( $\Omega^{-1}$ cm <sup>-1</sup> ) | $\chi_s$ (10°C)<br>( $\Omega^{-1}$ cm <sup>-1</sup> ) | $\chi_s$ (15°C)<br>( $\Omega^{-1}$ cm <sup>-1</sup> ) | $\chi_s$ (20°C)<br>( $\Omega^{-1}$ cm <sup>-1</sup> ) | $\chi_s$ (25°C)<br>( $\Omega^{-1}$ cm <sup>-1</sup> ) |
|---------------------------------|--|---|---|---|---|
| 0.0                             | $7.66 \cdot 10^{-3}$                                 | $8.87 \cdot 10^{-3}$                                  | 0.01012   | 0.01145   | 0.01282   |
| 0.05                            | $7.90 \cdot 10^{-3}$                                 | $9.14 \cdot 10^{-3}$                                  | 0.01044   | 0.01180   | 0.01322   |
| 0.1                             | $8.05 \cdot 10^{-3}$                                 | $9.31 \cdot 10^{-3}$                                  | 0.01063   | 0.01203   | 0.01347   |
| 0.5                             | $8.28 \cdot 10^{-3}$                                 | $9.58 \cdot 10^{-3}$                                  | 0.01094   | 0.01238   | 0.01386   |
| 1.0                             | $8.41 \cdot 10^{-3}$                                 | $9.72 \cdot 10^{-3}$                                  | 0.01111   | 0.01256   | 0.01407   |
| 2.0                             | $8.33 \cdot 10^{-3}$                                 | $9.63 \cdot 10^{-3}$                                  | 0.01100   | 0.01244   | 0.01394   |
| 3.0                             | $8.43 \cdot 10^{-3}$                                 | $9.75 \cdot 10^{-3}$                                  | 0.01114   | 0.01260   | 0.01411   |

observe the inverse phenomenon, because of the electrostatic repulsion of the anions and the fixed charges sites confined in the pore wall.

From Eq. (22), we can deduce the electroosmotic mobility profile within the membrane pore, which is presented in Fig. 4. In the absence of salt inside the membrane, the solvent flow is then only due to the counterions mobility. When the membrane is equilibrated with excess salt, the velocity profile becomes more homogeneous within the central region of the pore, because of the gradient concentration decreasing.

The electroosmotic conductivity  $\chi_s$  can also be deduced from the solvent velocity. In Table 2, we present the results obtained at different temperatures with all the experimental parameters. We have taken the

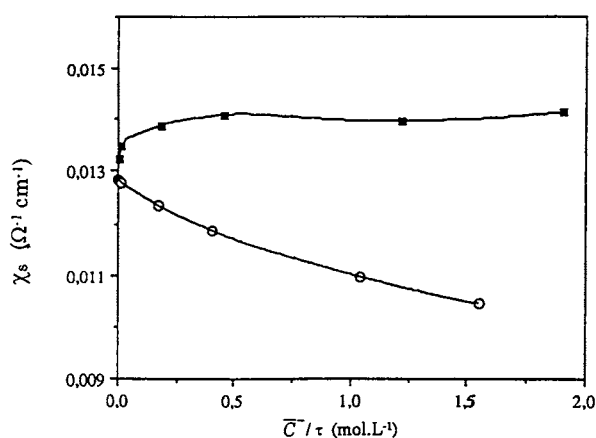


Fig. 5. Variation of the electroosmotic conductivity in a membrane pore at 25°C. (■): computation by taking the swelling parameters into account, (○): computation by using constant pore radius and surface charge density.

variation of the physicochemical constants with temperature into account, like the dielectric constant and the viscosity.<sup>(56)</sup> If we consider the swelling properties of the membrane, we observe that the conductivity slightly increases with the salt concentration inside the membrane (Fig. 5). The opposite effect is observed when we consider that the pore radius and the counterions concentration are constant. In fact, it is well known that electrokinetic phenomena are less important when the electrolyte concentration increases in confined media.<sup>(57)</sup> But for ion-exchange membranes, we must take the swelling properties of the polymer into account.

#### 4.2. Membrane Conductivity

In all experiments, the impedance diagrams were cutting the real axis at high frequencies (100 to 300 KHz), which allowed us to get directly the ohmic resistance of the membrane. Thus no impedance analysis was necessary to reach the membrane resistance, because of the high membrane conductivity and because of the cell geometry. The conductivity is then expressed as:

$$\chi_m = \frac{e}{RS} \quad (51)$$

where  $R$  is the membrane resistance and  $S$  the area of the sample. In order to get the experimental membrane pore conductivity, we use the following relation:

$$\chi_m^\tau = \frac{\chi_m}{\tau} \quad (52)$$

Then the membrane conductivity is modeled thanks to the theoretical determination of the electroosmotic conductivity  $\chi_s$ , and to the use of MSA transport theory. The fitting parameters are only the diffusion coefficients at infinite dilution of the added ions, and the diffusion coefficient of the counterion  $D_m$  which is defined as:

$$D_m = \frac{RT}{F^2} \lambda_m \quad (53)$$

We also write  $D_i^\circ$  as:

$$D_i^\circ = \frac{RT}{F^2} \lambda_i^\circ \quad (54)$$

We represent in Fig. 6 the variation of the membrane conductivity as a function of the salt concentration and temperature. In the experimental curves, we took the simulation of the electroosmotic conductivity  $\chi_e$  into account. We must however add that the electroosmosis contribution is relatively constant with electrolyte concentration, as we could observe it in the above section. Therefore, as a first approximation, the real experimental values of the membrane conductivity are only corrected with a constant value. We notice that the theoretical model obtained from MSA treatment is in good agreement with the experimental points. The fitting parameters are presented in Table 3 for each temperature. We have taken a mean diameter  $\sigma_a$  with a constant value of 3 Å, which should correspond to the sum of the cristallographic radii of the sodium and chlorure ions, which is about 2.8 Å.<sup>(56)</sup> This difference may be due to the ions hydratation which can also be different in confined media from that observed in electrolyte solutions. The lower curve was calculated using the limiting laws for the electrophoretic and relaxation corrections. This is the limit for point ions. The comparison with the MSA. treatment clearly exemply the influence of the size of the ions.

We also notice that the diffusion coefficients are much lower to those given in electrolyte solutions.<sup>(56)</sup> In fact, in confined media, it must exist

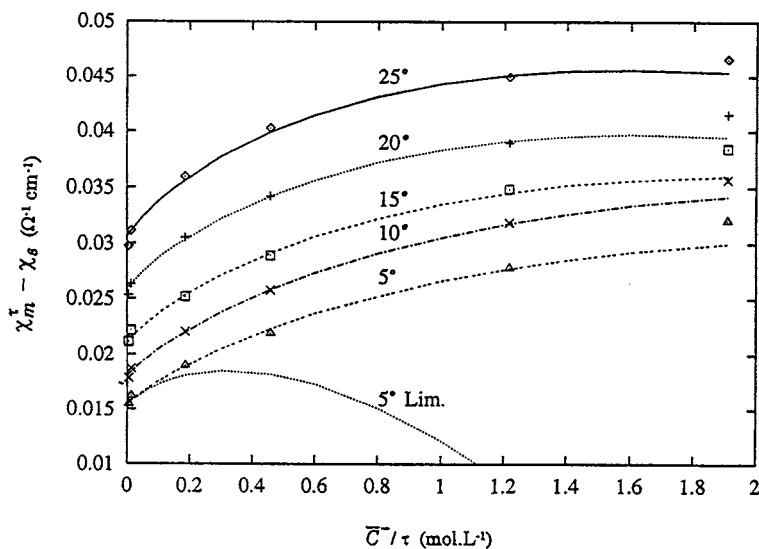


Fig. 6. Variation of the membrane conductivity by taking the simulation of the water flow in the membrane into account, with salt concentration at different temperatures. Comparison with MSA treatment. Lower curve: calculation using the limiting laws for the electrophoretic and relaxation terms.

**Table 3. Values of the Theoretical Parameters in Order to Model the Membrane Conductivity in the Framework of MSA Theory, with a Mean Diameter  $\sigma_s = 3 \text{ \AA}$**

| $T$<br>(°C) | $D_m(\times 10^5)$<br>( $\text{cm}^2 \text{ s}^{-1}$ ) | $D_+^o + D_-^o(\times 10^5)$<br>( $\text{cm}^2 \text{ s}^{-1}$ ) |
|-------------|--|--|
| 5.0         | 0.09   | 0.77   |
| 10.0        | 0.107  | 0.90   |
| 15.0        | 0.1271   | 1.0  |
| 20.0        | 0.1589   | 1.108  |
| 25.0        | 0.1915   | 1.26   |

friction effects between ions which implies lower values of the diffusion coefficients at infinite dilution.

### 4.3. Sodium Electrophoretic Mobility

In this work, electrophoretic mobility of sodium ion is determined by measuring the shifting of the radioactive tracer on Nafion 117 membrane sample under the action of an electric field. The electric migration in the membrane is then related to the ionic mobility  $u_i$  of the ion  $i$  which is in fact the velocity acquired per unit of applied electric field:

$$u_i = \frac{v_i}{E} \quad (55)$$

where  $E$  is the modulus of the applied electric field in the membrane. During a migration time  $t$ , the ionic species will have covered the apparent distance  $d_i$  defined as:

$$d_i = u_i E t \quad (56)$$

From Eq. (45), we can model the variation of the electrophoretic mobility of sodium ion in the membrane, as a function of salt concentration. The experimental values of the sodium mobility were obtained at 5°C. First, when there is no added salt in the membrane, the sodium ion has a mobility  $u_m$  which corresponds to the counterion mobility. By using the results obtained in the above section, we deduced a diffusion coefficient  $D_m$  of the counterion, which is directly related to the electric mobility  $u_m$ . However, this value was obtained by taking the solvent velocity into account. Then, to be in agreement with our model, all the experimental

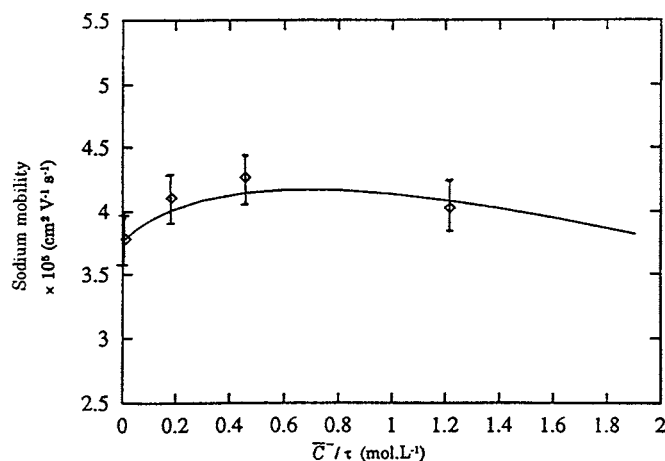


Fig. 7. Variation of the electrophoretic sodium mobility at 5°C with salt concentration. Comparison with MSA treatment by taking the water flow simulation into account.

values of the sodium mobility were taken away from a constant value, which in fact corresponds to the electroosmotic mobility at infinite dilution. We can notice that this mobility is related to the electroosmotic conductivity  $\chi_s$  by the relation:

$$\chi_s^\circ = F\bar{C}_m\hat{u}_s^\circ \quad (57)$$

Then, in order to model the experimental variation of the sodium mobility in the membrane, we used the following fitting parameters: a counterion mobility  $u_m$  equal to  $3.7510^{-5} \text{ cm}^2 \text{ V}^{-1} \text{ s}^{-1}$ , and a free cation mobility at infinite dilution  $u_+^\circ$  equal to  $1.5910^{-4} \text{ cm}^2 \text{ V}^{-1} \text{ s}^{-1}$  which corresponds to the half sum ( $D_+^\circ + D_-^\circ$ ) at 5°C (see Table 3). We represent in Fig. 7 the comparison between the experimental and the theoretical variation of the sodium mobility in the membrane, as a function of the salt concentration within the pore. The theoretical curve fits well over the experimental points by taking the experimental errors into account.

## 5. CONCLUSION

Experimental measurements of membrane conductivity and electrophoretic cation mobility can be related in order to understand the transport properties of ions in a ion-exchange membrane. Therefore, by using an equilibrium theory relatively simple like MSA, which is often used for electrolyte or polyelectrolyte solutions, we can also model the variation of the

transport coefficients in confined media. In this paper, we have chosen to take electrokinetic phenomena into account: by using the Poisson-Boltzmann equation, related to the Navier-Stokes equation, it is thus possible to simulate the solvent velocity within a membrane pore. More sophisticated density functional theory than Poisson-Boltzmann could be related to the Navier-Stokes equation. Moreover a better description of the one-particle and two-particle densities could be deduced. We hope to discuss this point in the future. In fact, it would be interesting to make experimental measurements of electroosmosis in order to compare directly the obtained results with out theoretical approach. Then, several parameters should be taken into account: the radius pore, the viscosity and the dielectric constant of the solvent or the pore geometry. For the physical properties of the solvent should be modified in confined media.

## ACKNOWLEDGMENTS

The authors thank gratefully N. Prulière, M. Périé, and J. Périé for their technical assistance.

## REFERENCES

1. A. Eisenberg and H. L. Yeager, *Perfluorinated Ionomer Membranes*, Am. Chem. Soc. Symposium Series, No. 180, Chapt. 14-19 (1982).
2. F. G. Will, *J. Electrochem. Soc.* **126**:36 (1979).
3. F. G. Will and H. S. Spacil, *J. Power Sources* **5**:173 (1980).
4. E. Gileadi, S. Srinivasan, F. J. Salzano, C. Braun, A. Beaufre, S. Gottesfeld, L. J. Nuttal, and A. B. LaConti, *J. Power Sources* **2**:191 (1977).
5. H. L. Yeager, B. Kipling, and R. L. Dotson, *J. Electrochem. Soc.* **127**:303 (1980).
6. R. S. Yeo, J. Mc Breen, G. Kissel, F. Kulesa, and S. Srinivasan, *J. Appl. Electrochem.* **10**:741 (1980).
7. K. Hass and P. Schmittinger, *Electrochim. Acta* **21**:1115 (1976).
8. J. Jorne, *J. Electrochem. Soc.* **129**:722 (1982).
9. M. W. Verbrugge and P. N. Pintauro, in B. F. Conway, R. E. White, and J. O'M. Bockris (Ed.), *Modern Aspects of Electrochemistry*, Vol. 19, Plenum Press, New York (1990).
10. S. W. Capece, P. N. Pintauro, and D. N. Bennion, *J. Electrochem. Soc.* **136**:10 (1989).
11. M. W. Verbrugge and R. F. Hill, *J. Phys. Chem.* **92**:6778 (1988).
12. M. W. Verbrugge and R. F. Hill, *J. Electrochem. Soc.* **137**(3):886 (1990).
13. A. Narebska and S. Koter, *Electrochim. Acta* **32**(3):449 (1987).
14. N. Smoluchowski, *Krak. Anz.* **182** (1903).
15. S. S. Dukhin and B. V. Derjaguin, *Surface and Colloid Science*, Vol. 7, Ed. Matijevic, John Wiley & Sons, New York (1974).
16. W. H. Koh, *J. Colloid Interface Sci.* **71**:613 (1979).
17. L. Dresner and K. A. Kraus, *J. Phys. Chem.* **67**:990 (1963).
18. L. Dresner, *J. Phys. Chem.* **67**:1635 (1963).
19. Y. Kobatake and H. Fujita, *J. Chem. Phys.* **40**:2212 (1964).
20. C. L. Rice and R. Whitehead, *J. Phys. Chem.* **69**:4017 (1965).

21. F. B. Hildebrand, *Advanced Calculus for Applications*, Prentice-Hall, Englewood Cliffs, New Jersey, p. 147 (1976).
22. F. A. Morriison, Jr. and J. F. Osterle, *J. Chem. Phys.* **43**:2111 (1965).
23. R. J. Gross and J. F. Osterle, *J. Chem. Phys.* **49**:228 (1968).
24. J. C. Fair and J. F. Osterle, *J. Chem. Phys.* **54**:3307 (1971).
25. R. L. Fleischer and P. B. Price, *Science* **140**:1221 (1963).
26. G. B. Westermann-Clark and J. L. Anderson, *J. Electrochem. Soc.* **130**:839 (1983).
27. W. Nernst, *Z. Phys. Chem.* **2**:613 (1888).
28. M. Planck, *Ann. Phys. Chem.* **39**:161 (1890).
29. L. Onsager, *Phys. Rev.* **37**:405 (1931).
30. L. Onsager, *Phys. Rev.* **38**:2265 (1931).
31. L. Onsager, *Ann. N.Y. Acad. Sci.* **46**:241 (1945).
32. H. L. Yeager and A. Steck, *Anal. Chem.* **51**:862 (1979).
33. A. Steck and H. L. Yeager, *Anal. Chem.* **51**: 1215 (1979).
34. A. Eisenberg and M. King, in R. S. Stein (Ed.), *Polymer Physics*, Academic Press, New York, Chapt. 4. (1977).
35. T. D. Gierke, *Proceedings of the Symposium on Perfluorocarbon Ion Exchange Membranes*, The Electrochemical Soc., Meeting, Georgia (1977).
36. G. Scibona, C. Fabiani, and B. Scuppa, *J. Membr. Sci.* **16**:37 (1983).
37. G. Pourcelly, A. Lindheimer, C. Gavach, and H. D. Hurwitz, *J. Electroanal. Chem.* **305**:97 (1991).
38. C. Gavach, P. Pamboutzoglou, M. Nedyalkov, and G. Pourcelly, *J. Membr. Sci.* **45**:37 (1989).
39. A. Narebska, S. Koter, and W. Kujawski, *J. Membr. Sci.* **25**:153 (1985).
40. H. L. Yeager, B. O'Dell, and Z. Twardowski, *J. Electrochem. Soc.* **129**(1): 85 (1982).
41. A. A. Gronowski and H. L. Yeager, *J. Electrochem. Soc.* **138**(9):2690 (1991).
42. A. Lindheimer, J. Molenat, and C. Gavach, *J. Electroanal. Chem.* **216**:71 (1987).
43. E. J. Taylor, N. R. K. Vilambi, R. Waterhouse, and A. Gelb, *J. Appl. Electrochem.* **21**:402 (1991).
44. T. D. Gierke, *The Electrochemical Society Extended Abstracts*, Vol. 77-2, Atlanta, GA, Abstract 438, p. 1139 (1977).
45. G. Gebel, P. Aldebert, and M. Pineri, *Polymer* **34**(2):333 (1993).
46. L. Belloni, M. Drifford, and P. Turq, *Chem. Phys.* **83**:147 (1984).
47. W. G. Mc Millan and J. E. Mayer, *J. Chem. Phys.* **13**:276 (1945).
48. E. Waisman and J. L. Lebowitz, *J. Chem. Phys.* **52**:4307 (1970).
49. L. Blum, *Mol. Phys.* **30**(5):1529 (1975). L. Blum and J. S. Høye, *J. Phys. Chem.* **81**:1311 (1977). K. Hiroike, *Mol. Phys.* **33**:1195 (1977).
50. M. Périé and J. Périé, *J. Electroanal. Chem.* **393**:17 (1995).
51. S. Rossy-Delluc, T. Cartailier, P. Turq, O. Bernard, N. Morel-Desrosiers, J. P. Morel, and W. Kunz, *J. Phys. Chem.* **97**:5136 (1993).
52. P. Turq, L. Orcil, J. P. Simonin, and J. Barthel, *Pure Appl. Chem.* **59**:1083 (1987).
53. L. Orcil, P. Turq, C. Musikas, Y. Prulière, and M. Chemla, *J. Phys. Chem.* **88**:5265 (1984).
54. O. Bernard, P. Turq, et L. Blum, *J. Phys. Chem.* **95** (1991) 9508.
55. O. Bernard, W. Kunz, P. Turq, et L. Blum, *J. Phys. Chem.* **96**:3833 (1992). P. Turq, L. Blum, O. Bernard and W. Kunz, *J. Phys. Chem.* **99**:822 (1995). A. Chhah, P. Turq, O. Bernard, J. M. G. Barthel and L. Blum, *Ber. Bunsenges. Phys. Chem.* **12**:1516 (1994).
56. R. A. Robinson and R. H. Stokes, *Electrolyte Solutions*, 2nd Ed., Butterworth, London (1959).
57. H. Helmholtz, *Wied. Ann.* **7**:337 (1879).